Journal of Physics: Conference Series

PAPER • OPEN ACCESS

Using Spin Observables and Polarizations to Probe Top-Higgs FCNC Couplings at Colliders

To cite this article: Blaženka Meli and Monalisa Patra 2017 *J. Phys.: Conf. Ser.* **878** 012026

IOP Conf. Series: Journal of Physics: Conf. Series **878** (2017) 012026 doi:10.1088/1742-6596/878/1/012026

Using Spin Observables and Polarizations to Probe Top-Higgs FCNC Couplings at Colliders

Blaženka Melić[1], **Monalisa Patra**[2]

Rudjer Bošković Institute, Department of Theoretical Physics, Bijenička 54, HR-10000 Zagreb, Croatia

E-mail: [1]melic@irb.hr,[2]mpatra@irb.hr

Abstract. We present how the polarized linear colliders can be used, complementary to the LHC, to fully determine the top-Higgs flavor changing neutral current (FCNC) couplings by using produced asymmetries and top spin polarizations and correlations.

1. The flavor changing top quark couplings at hadron colliders

The discovery of the Higgs boson at the LHC, has lead to a dedicated program of measuring its various properties so as to look for deviations from the standard model (SM). In the SM the presence of a single Higgs doublet leads to no FCNC transitions at tree level mediated by the Higgs boson. For e.g. the SM branching ratio of $t \to cH$ is extremely small, of the order $\mathrm{BR}(t \to cH)_{\mathrm{SM}} \approx 10^{-15}$ [1, 2], which is many orders of magnitude smaller than the value to be measured at the LHC at 14 TeV. Therefore an affirmative observation of the process $t \to qH$, well above the SM rate, will be a conclusive indication of new physics beyond the SM. Limits on the FCNC couplings in the light quark-Higgs sector can be obtained from neutral meson oscillations ($K^0 - \bar{K}^0$, $B^0 - \bar{B}^0$ and $D^0 - \bar{D}^0$) [3].

The most general FCNC tqH Lagrangian considered is of the form

$$\begin{aligned} \mathcal{L}^{tqH} &= g_{tu}\bar{t}_R u_L H + g_{ut}\bar{u}_R t_L H + g_{tc}\bar{t}_R c_L H + g_{ct}\bar{c}_R t_L H + h.c \\ &= \bar{t}(g_{qt}P_R + g^*_{tq}P_L)qH + \bar{q}(g_{tq}P_R + g^*_{qt}P_L)tH. \end{aligned} \quad (1)$$

The total decay width of the top in the presence of these FCNC couplings is then

$$\Gamma_t = \Gamma_t^{SM} + \Gamma_{t\to q_H} \approx \Gamma_t^{SM} + 0.155\,(\mid g_{tq} \mid^2 + \mid g_{qt} \mid^2)\,, \quad (2)$$

where the width $\Gamma_t^{SM} = \Gamma_{t\to W^+b} = 1.35$ GeV, for $m_t = 173.3$ GeV at NLO, while the experimentally observed value of the total top-quark width is $\Gamma_t = 1.41^{+0.19}_{-0.15}$ GeV. The additional FCNC decay processes give positive contributions to Γ_t, proportional to $(\mid g_{tq} \mid^2 + \mid g_{qt} \mid^2)$ and from the experimentally observed Γ_t an upper bound on $\sqrt{\mid g_{tq} \mid^2 + \mid g_{qt} \mid^2}$ can be obtained. The ATLAS and the CMS collaborations have set upper limits on the tqH coupling through the top pair production, with one top decaying to Wb and the other top assumed to decay to qH. The 95% CL upper limit obtained by ATLAS by combining the analysis of the different Higgs decay channel, at $\sqrt{s} = 8$ TeV and an integrated luminosity of 20.3 fb^{-1} are $\mathrm{Br}(t \to cH) \leq 4.6 \times 10^{-3}$ and $\mathrm{Br}(t \to uH) \leq 4.5 \times 10^{-3}$ [4, 5]. It was shown in Ref. [6], that studying the single top

+ Higgs production in $pp \to (t \to W^+b)H$ at the LHC, will lead to the disentangling of the tuH and tcH couplings. They analysed in detail the multilepton, diphoton plus lepton and vector boson plus Higgs final state and obtained bounds on the FCNC couplings. They found the lepton rapidity distribution from the multilepton searches improve the bounds obtained on BR(t $\to$ uH) by a factor of 1.5 and that they can be used to discriminate between the tcH and tuH couplings.

2. Analysis of the tqH final state in the polarized e^-e^+ linear collider

The tqH coupling has also been studied in the context of the next generation e^-e^+ linear colliders, the International Linear Collider (ILC) and the Compact Linear Collider (CLIC) [7, 8]. The baseline machine design for both the colliders allows for up to $P^{L,T}_{e^-} = \pm 80\%$ electron (longitudinal and transversal) polarization, while provisions have been made to allow positron polarization of $P^{L,T}_{e^+} = \pm 30\%$ as an upgrade option. Both these machines are designed to operate at centre of mass energies of 350, 500 and 1000 GeV, with the possibility of CLIC to be also adapted for the 3 TeV operation.

We study the $t\bar{t}$ production in the context of the e^-e^+ linear collider as

$$\begin{aligned} e^-(p_1) + e^+(p_2) \to t(q_1) + \bar{t}(q_2), \\ t(q_1) \to q(p_q) + H, \qquad \bar{t}(q_2) \to \bar{b}(p_b) + l^+(p_l) + \nu(p_\nu). \end{aligned} \tag{3}$$

where $q = u, c$.

The total phase space for the process under study is split into the product of the differential cross-section for the $t\bar{t}$ production, the three-particle decay of the anti-top quark and the two-particle decay of the top quark, with the Higgs decaying to $b\bar{b}$. The analytical analysis is done first considering the decay of t to qH along with the inclusive decay of $\bar{t}$. The dominant SM background to this process is also considered, with the inclusive decay of $\bar{t}$ and the SM decay of top to W^+b, with the W decaying hadronically. The total squared matrix element $\mid \bar{\mathcal{M}}^2 \mid$ of the process in (3) is defined as

$$\mid \bar{\mathcal{M}}^2 \mid \;=\; \sum_{L,R} \sum_{(\lambda_t \lambda_t' = \pm)} \rho^{P t\bar{t}}_{LR,\lambda_t\lambda_t'} \rho^{D^t}_{\lambda_t\lambda_t'} = \sum_{L,R} \sum_{(\lambda_t \lambda_t' = \pm)} \mathcal{M}^{L,R}_{\lambda_t} \mathcal{M}^{*L,R}_{\lambda_t'} \rho^{D^t}_{\lambda_t\lambda_t'}, \tag{4}$$

where $\mathcal{M}^{L,R}_{\lambda_t}$ is the production helicity amplitude of the top with a given helicity λ_t. The helicities of the anti-top are summed over. The decay matrix of the top along with the production helicity amplitudes are listed in the Appendix of Ref. [9]. Our calculations are done in the frame where the electron beam direction is in the positive z direction, with the top emitted at a polar angle θ_t and the quark emitted in the top decay makes a polar θ_q angle with the electron beam. The four-vector in the rest frame of the top are related to the c.m. frame by boosting in the z direction and rotating around the y axis.

Combining the production and the density matrices in the narrow width approximation for t, we get the polar distribution of the emitted quark q in the presence of the beam polarization, after integrating over ϕ_q, θ_t, to be

$$\frac{d\sigma}{ds \; d\cos\theta_q \; d\phi_t} \;=\; |T|^2 , \tag{5}$$

where the most general formula for the matrix element square $|T_{e^-e^+}|^2$ for arbitrary polarized e^-e^+ beams is given in [10, 11] as

$$\begin{aligned} |T|^2 \;=\; \frac{1}{4} \Big\{ & (1 - P^L_{e^-})(1 + P^L_{e^+}) |T_{e^-_L e^+_R}|^2 + (1 + P^L_{e^-})(1 - P^L_{e^+}) |T_{e^-_R e^+_L}|^2 \\ & - 2 P^T_{e^-} P^T_{e^+} \mathrm{Re}\; \mathrm{e}^{\mathrm{i}(\eta - 2\phi_t)} \mathrm{T}^*_{\mathrm{e^-_R e^+_L}} \mathrm{T}_{\mathrm{e^-_L e^+_R}} \Big\} , \end{aligned} \tag{6}$$

where $\eta = \alpha_- + \alpha_+$, with $\alpha_\mp$ denoting the angle of polarization of the electron and the positron, respectively. In Eq. (6) $T_{e^-_{\lambda_1} e^+_{\lambda_2}}$ is the helicity amplitude for the process under consideration and λ_1, λ_2 are the helicities of the electron and the positron, respectively. The degree of the longitudinal and the transversal polarization for the electrons and positrons are denoted by $P^L_{e^\mp}$ and $P^T_{e^\mp}$, respectively, and particular pieces $|T_{e^-_L e^+_R}|^2$, $|T_{e^-_R e^+_L}|^2$ and $T^*_{e^-_R e^+_L} T_{e^-_L e^+_R}$ are given by

$$\begin{aligned} |T_{e^\mp_L e^\pm_R}|^2 &= (|g_{tq}|^2 + |g_{qt}|^2)\left(a_0 + a_1 \cos\theta_q + a_2 \cos^2\theta_q\right) \\ &\quad \pm(|g_{tq}|^2 - |g_{qt}|^2)\left(b_0 + b_1 \cos\theta_q + b_2 \cos^2\theta_q\right) , \\ T^*_{e^-_R e^+_L} T_{e^-_L e^+_R} &= (3\cos^2\theta_q - 1)\cos(\eta - 2\phi_t)\left\{(|g_{tq}|^2 + |g_{qt}|^2)c_0 + (|g_{tq}|^2 - |g_{qt}|^2)d_0\right\} , \end{aligned} \quad (7)$$

where a_i, b_i, c_0, d_0 coefficients are functions of the standard SM γ and Z couplings with the top and the leptons in the $t\bar{t}$ production. These equations are explicitly given in Ref. [9]. The Yukawa chiral couplings $|g_{tq}|^2$ and $|g_{qt}|^2$ are found to be proportional to the polar angle of the emitted light quark, $\cos\theta_q$ and $\cos^2\theta_q$, but those dependences differ for $|g_{tq}|^2$ and $|g_{qt}|^2$. This makes possible to control the influence of the individual chiral couplings with a suitable choice of beam polarization.

3. Asymmetries and top spin observables at the ILC

We study different distributions in the presence of chiral FCNC couplings and accordingly construct asymmetries to set limits on them. We perform our analysis considering $\sqrt{|g_{tq}|^2 + |g_{qt}|^2} = 0.16$, in accordance with the latest LHC bounds [6]. The background i.e. the SM $\bar{t}Wb$ contribution is scaled down, to be compared with the signal. For analytical results we are not applying any cuts on the final state, but a detailed analysis using all the experimental cuts is performed in the full numerical simulation.

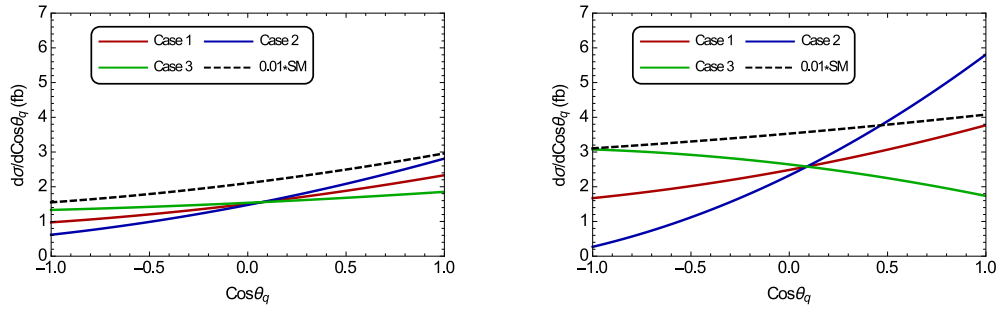

Figure 1: The polar angle distribution of the quark at $\sqrt{s} = 500$ GeV, for (a) $P^L_{e^-} = P^L_{e^+} = 0$ and (b) $P^L_{e^-} = -0.8$, $P^L_{e^+} = 0.3$. The different Cases are discussed in the text.

The polar angle distribution of the emitted quark, calculated from Eqs.(5-7), is plotted in Fig. 1 for both the signal and the background, for (a) $P^L_{e^-} = P^L_{e^+} = 0$ and (b) $P^L_{e^-} = -0.8$, $P^L_{e^+} = 0.3$. As we can see the polar angle distribution is sensitive to the chirality of the Yukawa couplings and the results are given for three different cases:

- Case 1 : $\sqrt{|g_{tq}|^2 + |g_{qt}|^2} = 0.16$
- Case 2 : $\sqrt{|g_{tq}|^2 + |g_{qt}|^2} = 0.16$, with $|g_{qt}|^2 = 0$
- Case 3 : $\sqrt{|g_{tq}|^2 + |g_{qt}|^2} = 0.16$, with $|g_{tq}|^2 = 0$.

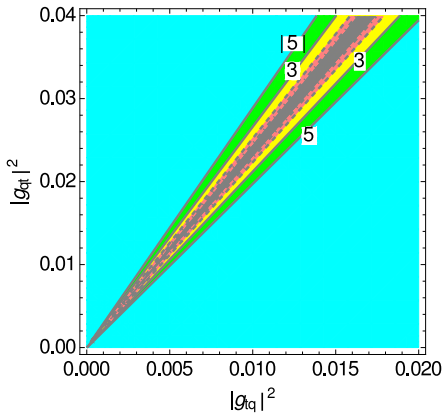

Figure 2: Contour plots of 3σ and 5σ statistical significance in the $|g_{tq}|^2 - |g_{qt}|^2|$ region from A_{fb} for $\theta_0 = 0$. The solid lines are for the unpolarized case, the dashed lines are for $P^L_{e^-}$ = -0.8, $P^L_{e^+} = 0.3$. See text for explanation.

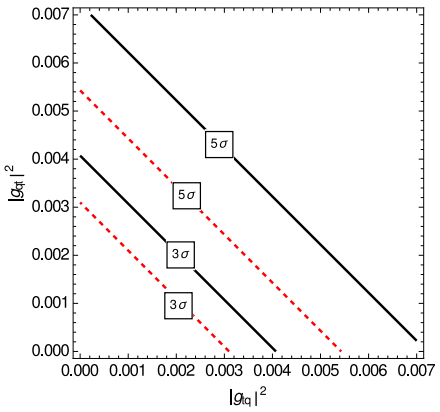

Figure 3: Contour plots in the $|g_{tq}|^2 - |g_{qt}|^2$ plane, for the statistical significance S, from the production cross section, with unpolarized beams [black] and a beam polarization of $P^L_{e^-}$ = -0.8 and $P^L_{e^+} = 0.3$ [red-dashed].

The different Cases behave similar in the unpolarized case, Fig. 1a. For polarized beams all Cases clearly differ among each other, Fig. 1b. Therefore the manifestation of the dominance of one of the coupling, if present, will be prominent using the suitable initial beam polarization.

In the following, we also perform a full numerical simulation of the FCNC interactions in the $t \to qH$ decay at the ILC. The detailed analysis can be found in Ref. [9]. The various distributions which we consider are calculated in the $t\bar{t}-$ zero momentum frame (ZMF). The decay products, which act as spin analyzers for our case are the non-b jet (q) from the decay $t \to qH$ and the lepton (l^-) from the decay $\bar{t} \to l^-\bar{\nu}\bar{b}$. All the distribution plots are given with the number of surviving events, for $\mathcal{L} = 500$ fb^{-1} and energies $\sqrt{s} = 500$ GeV.

3.1. Constraints on the chiral FCNC couplings by angular asymmetries

Using the above fact that the couplings are sensitive to the polar angle distributions of the quark, we have also considered different asymmetries, the forward-backward asymmetry (FB) and the azimuthal asymmetry, which can be used to give simultaneous limits on both of the couplings [9]. While the FB asymmetry gives a clear distinction among the different cases, as illustrated in Sec. 3, the azimuthal asymmetry exhibits similar behavior for the signal as well as for the background and therefore cannot be an useful observable.

The limits on the FCNC couplings from the FB asymmetry,A_{fb}, are given in Fig. 2 where we show the $|g_{tq}|^2 - |g_{qt}|^2|$ region which can be probed at a statistical significance of 3σ and 5σ, with both unpolarized and polarized beams. The region in blue will be probed at 5σ and green+blue areas will be explored at 3σ with unpolarized beams. The inclusion of the beam polarization probes yellow+green+blue areas at 5σ and pink+yellow+green+blue at 3σ. The region which can not be probed by ILC with this choice of beam polarization is shown in grey. The outside area surrounding solid lines can be probed with unpolarized beams and the outside area surrounding dashed lines can be probed with a beam polarization of $P^L_{e^-} = -0.8$, $P^L_{e^+} = 0.3$. Obviously, the inclusion of beam polarization can probe a greater region in the $|g_{tq}|^2 - |g_{qt}|^2$ parameter space.

We also estimate the sensitivity that can be obtained for the FCNC tqH couplings, given

by the efficient signal identification and the significant background suppression which can be achieved at the linear collider. In Fig. 3 we present the contours of 3σ and 5σ significance for our process in the $|g_{tq}|^2 - |g_{qt}|^2$ plane from the production cross section. The sensitivity of the linear collider will increase with the implementation of beam polarization with left polarized electrons and right polarized positrons. One can see that at 3σ of statistical significance and $\mathcal{L}$ = 500 fb^{-1}, $\sqrt{|g_{tq}|^2 + |g_{qt}|^2}$ can be probed to 0.063 (0.056) with unpolarized (polarized) beams. The limits obtained from the asymmetries, specially A_{fb} from Fig.2 will be more stronger and will not be symmetric in the $|g_{tq}|^2 - |g_{qt}|^2$ plane.

3.2. Constraints on the chiral FCNC couplings by top spin observables

The top(antitop)-quark polarization and spin-spin correlations can be measured using the double differential angular distribution of the top and antitop quark decay products:

$$\frac{1}{\sigma}\frac{d^2\sigma}{d\cos\theta_f d\cos\theta_{\bar{f}}} = \frac{1}{4}\left(1 + B_t\cos\theta_f + B_{\bar{t}}\cos\theta_{\bar{f}} - C\cos\theta_f\cos\theta_{\bar{f}}\right)\,, \tag{8}$$

where $\theta_f(\theta_{\bar{f}})$ is the angle between the direction of the top (antitop) spin analyser f, ($\bar{f}$) in the t ($\bar{t}$) rest frame.

We consider the following spin observables

$$\begin{aligned}
\mathcal{O}_1 &= \frac{4}{3}\mathbf{S}_t\cdot\mathbf{S}_{\bar{t}}\,,\\
\mathcal{O}_2 &= \mathbf{S}_t\cdot\hat{\mathbf{a}}, \qquad \bar{\mathcal{O}}_2 = \mathbf{S}_{\bar{t}}\cdot\hat{\mathbf{b}}\,,\\
\mathcal{O}_3 &= 4(\mathbf{S}_t\cdot\hat{\mathbf{a}})(\mathbf{S}_{\bar{t}}\cdot\hat{\mathbf{b}}),\\
\mathcal{O}_4 &= 4\left((\mathbf{S}_t\cdot\hat{\mathbf{p}})(\mathbf{S}_{\bar{t}}\cdot\hat{\mathbf{q}}) + (\mathbf{S}_t\cdot\hat{\mathbf{q}})(\mathbf{S}_{\bar{t}}\cdot\hat{\mathbf{p}})\right),
\end{aligned} \tag{9}$$

giving the net spin polarization of the top-antitop system ($\mathcal{O}_1$), polarization of the top (antitop) quark ($\mathcal{O}_2(\bar{\mathcal{O}}_2)$), the top-antitop spin correlation ($\mathcal{O}_3$), with respect to spin quantization axes $\hat{\mathbf{a}}$ and $\hat{\mathbf{b}}$. The observable $\mathcal{O}_4$ is an additional top-antitop spin correlation with respect to the momentum of the incoming and the outgoing particles [12]. We have

$$\begin{aligned}
B_t &= \langle\mathcal{O}_2\rangle\,\kappa_f\,, \qquad B_{\bar{t}} = \langle\bar{\mathcal{O}}_2\rangle\,\kappa_{\bar{f}}\,,\\
C &= \langle\mathcal{O}_3\rangle\,\kappa_f\kappa_{\bar{f}}\,.
\end{aligned} \tag{10}$$

Since there is no CP violation in our case, we consider $B \equiv B_t = \mp B_{\bar{t}}$ for $\hat{\mathbf{a}} = \pm\hat{\mathbf{b}}$. Here $\kappa_q(\kappa_{l^-})$ are the top, anti-top spin analysers. The spin analyser for the FCNC top-Higgs decays can be either a direct t-quark daughter, i.e. H or c/u-quark, or H decay products like b or $\bar{b}$ in $b\bar{b}$ decay, or $\tau^+(\tau^-)$ in $H \to \tau^+\tau^-$ decay, or jets. On the other hand, the spin analyser for $\bar{t}$ are W^- or $\bar{b}$, or a W^- decay products $l^-, \bar{\nu}$ or jets. We consider the c/u quark from the top and the l^- from the anti-top as spin analysers in this work.

The top spin analyzing power of q (κ_q) from the $t \to Hq$ decay, b quark (κ_b), from the top decay to W^+b and the lepton from the top decay to $l^+\nu b$ is

$$\kappa_q = \frac{|g_{qt}|^2 - |g_{tq}|^2}{|g_{qt}|^2 + |g_{tq}|^2}, \quad \kappa_b = \frac{m_t^2 - 2m_W^2}{m_t^2 + 2m_W^2}, \quad \kappa_l = 1. \tag{11}$$

The leptons emitted from the top decay, due to the $V-A$ interactions are the perfect top spin analysers, $\kappa_l = 1$, (α_s corrections are negligible), with their flight directions 100% correlated with the directions of the top spin. It is clear from Eq. (11) that with $|g_{qt}|^2 \simeq |g_{tq}|^2$, the spin

information of the top will be lost ($\kappa_q \approx 0$). However, in the presence or dominance of only one of the coupling, the emitted quark acts as a perfect spin analyser ($\kappa_q \approx 1$).

The observable $\mathcal{O}_1$ can be probed using the opening angle distribution (φ), i.e. the angle between the direction of flight of the two (top and antitop) spin analysers, defined in the t and $\bar{t}$ frames, respectively, i.e $\hat{\mathbf{p}}_q \cdot \hat{\mathbf{p}}_l = \cos\varphi$.

$$\frac{1}{\sigma}\frac{d\sigma}{d\cos\varphi} = \frac{1}{2}\left(1 - D\cos\varphi\right), \qquad D = \langle\mathcal{O}_1\rangle\,\kappa_q\kappa_{l^-} \tag{12}$$

The arbitrary unit vectors $\hat{\mathbf{a}}$ and $\hat{\mathbf{b}}$ in (9) specify different spin quantization axes which can be chosen to maximize the desired polarization and the correlation effects, and we take them as

$$\begin{aligned}
&\hat{\mathbf{a}} = -\hat{\mathbf{b}} = \hat{\mathbf{q}}\,, && (\text{“helicity” basis})\,,\\
&\hat{\mathbf{a}} = \hat{\mathbf{b}} = \hat{\mathbf{p}}\,, && (\text{“beamline” basis})\,,\\
&\hat{\mathbf{a}} = \hat{\mathbf{b}} = \hat{\mathbf{d}}_{\mathbf{SM}} = \hat{\mathbf{d}}^{\max}_{\rm SM} = \frac{-\hat{\mathbf{p}} + (1-\gamma)z\;\hat{\mathbf{q}}_1}{\sqrt{1-(1-\gamma^2)z^2}}\,, && (\text{“off}-\text{diagonal” basis})\,,
\end{aligned} \tag{13}$$

where $\hat{\mathbf{q}} = \hat{\mathbf{q}}_1$ is the direction of the outgoing top quark and $\hat{\mathbf{p}}$ is the direction of the incoming beam, both in the $t\bar{t}$ center of mass frame. The off-diagonal basis [13] is the one, where the top spins are 100% correlated ($z = \hat{\mathbf{p}}\cdot\hat{\mathbf{q}}_1 = \cos\theta$ and $\gamma = E_t/m_t = 1/\sqrt{1-\beta^2}$) and which interpolates between the beamline basis at the threshold ($\gamma \to 1$) and the helicity basis for ultrarelativistic energies ($\gamma \to \infty$). We would like to point out here that this off-diagonal basis $\hat{\mathbf{d}}_{\rm SM}$ is specific to the SM $t\bar{t}$ production, but a general procedure for finding such an off-diagonal basis for any model is given in [14, 15, 16]. The complementary basis to the “off-diagonal” one, where the correlation of the top-antitop spins is minimal can be found in Refs. [9, 16].

In Table 1 we present the values of the different spin observables in the different spin basis considered here, in the presence of beam polarizations. We note that the top (antitop) spin

Table 1: The value of the spin observables in different bases, with different choices of initial beam polarization.

Observables	Basis	$P^L_{e^-}=0, P^L_{e^+}=0$	$P^L_{e^-}=0.8, P^L_{e^+}=-0.3$	$P^L_{e^-}=-0.8, P^L_{e^+}=0.3$
$\mathcal{O}_1$		$0.333\kappa_f$	$0.333\kappa_f$	$0.333\kappa_f$
	hel	$-0.076\kappa_f$	$0.247\kappa_f$	$-0.239\kappa_f$
	beam	$-0.174\kappa_f$	$0.344\kappa_f$	$-0.436\kappa_f$
$\mathcal{O}_2$	off	$0.176\kappa_f$	$-0.351\kappa_f$	$0.443\kappa_f$
	hel	$-0.654\kappa_f$	$-0.666\kappa_f$	$-0.648\kappa_f$
	beam	$0.881\kappa_f$	$0.852\kappa_f$	$0.897\kappa_f$
$\mathcal{O}_3$	off	$0.911\kappa_f$	$0.886\kappa_f$	$0.924\kappa_f$
$\mathcal{O}_4$		$0.546\kappa_f$	$0.612\kappa_f$	$0.512\kappa_f$

polarizations are quite sensitive to the beam polarization, while this is not the case for the spin-spin correlations $\mathcal{O}_3, \mathcal{O}_4$ where the influence of the beam polarizations gets diluted. Also note that all observables are proportional to $\kappa_f = \kappa_q$ and will be equal to zero if g_{tq} and g_{qt} are equal.

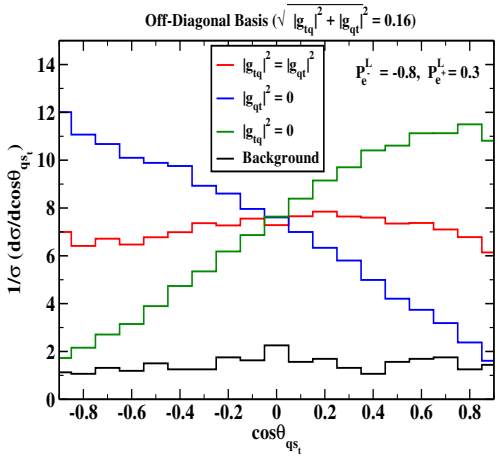

Figure 4: The normalized distribution with polarized beams, θ_{qs_t} is the angle between the direction of the top spin analyzer (q from $t \to qH$) in t rest frame and the spin quantization axis of the top (s_t) in $t\bar{t}$ZMF.

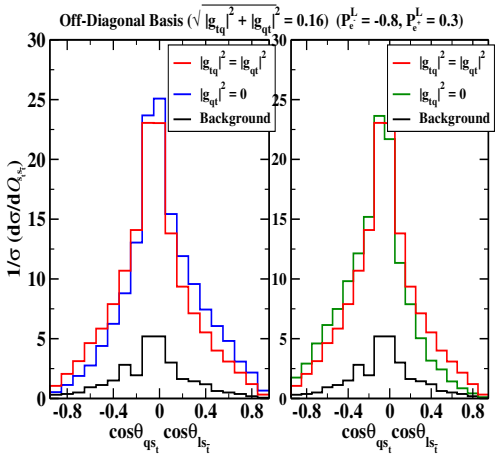

Figure 5: The normalized distribution of the product $\cos\theta_{qs_t}\cos\theta_{ls_{\bar{t}}}$, ($\theta_{qs_t} = \angle(\hat{\mathbf{p}}_q, \hat{\mathbf{a}}), \theta_{qs_{\bar{t}}} = \angle(\hat{\mathbf{p}}_l, \hat{\mathbf{b}})$), using the off-diagonal basis, at $\sqrt{s} = 500$ GeV, with polarized beams and $\mathcal{L} = 500$ fb^{-1}.

The top spin ($\sim \langle\mathcal{O}_2\rangle$) is considered in the normalized distribution $1/\sigma(d\sigma/d\cos\theta_{qs_t})$, where θ_{qs_t} is the angle between the direction of the top spin analyzer (non-b jet) in the top rest frame and the top spin quantization axis (s_t) in the $t\bar{t}$-ZMF. The angle $\cos\theta_{qs_t}$ is the angle $\cos\theta_f$ defined in Eq. (8). The spin of the top can be chosen in the direction of any of the spin quantization axes as defined in Eq.(13). The 'beamline' basis and the 'off-diagonal' basis, Fig. 4, are most sensitive to the top polarization and therefore also to the decay dynamics of the top. The chiral nature of the FCNC coupling will be more clearly visible in these two basis, with a flat distribution in case of the equality of the two chiral coupling. The effect is further enhanced with the beam polarizations of $P^L_{e^-} = -0.8$ and $P^L_{e^+} = 0.3$, in all the spin bases considered here.

The double differential angular distribution of the top and the antitop defined in Eq. (8) provides a measurement of the spin-spin correlations ($\sim \langle\mathcal{O}_3\rangle$). It was shown in Ref. [17] that, for the experimental analysis, it is more suitable to use the one-dimensional distribution of the product of the cosines, $\mathcal{O}_{s_t,s_{\bar{t}}} = \cos\theta_f \cos\theta_{\bar{f}}$, rather than analyzing the distribution in (8). We define $\cos\theta_f\cos\theta_{\bar{f}}$ as $\cos\theta_{qs_t}\cos\theta_{ls_{\bar{t}}}$ for our analysis. The $1/\sigma(d\sigma/d\mathcal{O}_{s_t,s_{\bar{t}}})$ distribution is shown in Fig. 5, using the 'off-diagonal' basis and a longitudinal beam polarization of $P^L_{e^-} = -0.8$ and $P^L_{e^+} = 0.3$. The asymmetry of the plot around $\cos\theta_{qs_t}\cos\theta_{ls_{\bar{t}}} = 0$, although not large, signals for the spin-spin correlation. The plot for Case 2 ($|g_{qt}|^2 = 0$) shows more events for positive values for $\cos\theta_{qs_t}\cos\theta_{ls_{\bar{t}}}$, whereas for Case 3 ($|g_{tq}|^2 = 0$) one gets more events for negative values of $\cos\theta_{qs_t}\cos\theta_{ls_{\bar{t}}}$.

4. Conclusion

We have been able to show that at linear colliders one can explore the chiral structure of the flavor-violating top-Higgs interactions in the $t\bar{t}$ production, using different beam polarizations and various top spin observables. The chiral nature of these couplings is not evident from the measurements made at the LHC as both the branching ratio of the top to qH and the total production cross section are proportional to $|g_{tq}|^2 + |g_{qt}|^2$.

The possibility of the adjustment of the initial beam polarization, leads to an enhancement of the sensitivity of the measured branching ratios and the asymmetries on the FCNC parameters. The various angular distributions of the top decay products are related to the top spin

observables, whose effect can be increased with a suitable choice of spin quantization axis. The quark emitted from the top FCNC decay, acts as a perfect spin analyzer ($\kappa_q = 1$)in the presence of a single chiral coupling, and the correlation is completely lost when $|g_{tq}|^2 = |g_{qt}|^2$. The off-diagonal basis along with the beamline basis is found to be most sensitive to the chirality of the coupling with its effect being enhanced with a suitable choice of beam polarization.

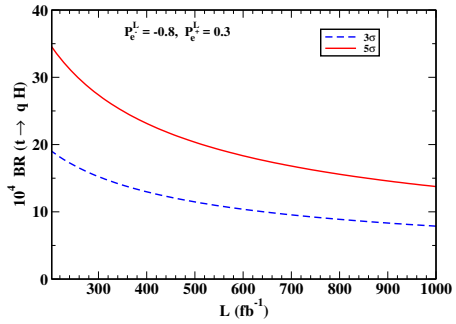

Figure 6: The sensitivity of 3σ and 5σ to BR($t \to qH$) at $\sqrt{s}$ = 500 GeV, as a function of the luminosity, $\mathcal{L}$.

We have performed a detailed analysis, applying all the relevant cuts at the linear collider and obtain a limit on the couplings from the total cross section. The 3σ and the 5σ upper bounds on the branching ratios, which can be obtained at the ILC, at $\sqrt{s} = 500$ GeV, with the choice of beam polarization $P_{e^-}^L = -0.8$, $P_{e^+}^L = 0.3$ are shown in Fig. 6.

We find that BR($t \to qH$) can be probed to $5.59 \times 10^{-3}(8.84 \times 10^{-4})$ at 3σ level at the ILC, with $\sqrt{s} = 500$ GeV, $\mathcal{L} = 500$ fb^{-1} and a beam polarization of $P_{e^-}^L = 0(-0.8), P_{e^+}^L = 0(0.3)$.

Acknowledgement
B.M. would like to thank the organizers for the invitation and organizing the pleasant conference. This work is supported by the Croatian Science Foundation (HRZZ) project PhySMaB, 'Physics of Standard Model and Beyond' as well as by the H2020 Twinning project No. 692194, RBI-T-WINNING.

References

[1] Mele B, Petrarca S and Soddu A, *Phys. Lett.* B **435**, 401 (1998) (*Preprint* hep-ph/9805498)
[2] Aguilar-Saavedra J A, *Acta Phys. Polon.* B **35**, 2695 (2004) (*Preprint* hep-ph/0409342)
[3] Blankenburg G, Ellis J and Isidori G, *Phys. Lett.* B **712**, 386 (2012) (*Preprint* arXiv:1202.5704 [hep-ph])
[4] CMS Collaboration [CMS Collaboration], (*CMS-PAS-HIG*-13-034)
[5] Aad G *et al.* [ATLAS Collaboration], JHEP **1512**, 061 (2015) (*Preprint* arXiv:1509.06047 [hep-ex])
[6] Greljo A, Kamenik J F and Kopp J, JHEP **1407**, 046 (2014) (*Preprint* arXiv:1404.1278 [hep-ph])
[7] Han T, Jiang J and Sher M, *Phys. Lett.* B **516**, 337 (2001) (*Preprint* hep-ph/0106277)
[8] Hesari H, Khanpour H and Najafabadi M M, *Phys. Rev.* D **92**, no. 11, 113012 (2015) (*Preprint* arXiv:1508.07579 [hep-ph])
[9] Melić B and Patra M, JHEP **1701**, 048 (2017) (*Preprint* arXiv:1610.02983 [hep-ph])
[10] Kleiss R, *Z. Phys.* C **33**, 433 (1987).
[11] Hikasa K , *Phys. Rev.* D **33**, 3203 (1986).
[12] Brandenburg A, Flesch M and Uwer P, *Phys. Rev.* D **59**, 014001 (1999) (*Preprint* hep-ph/9806306)
[13] Parke S J and Shadmi Y, *Phys. Lett.* B **387**, 199 (1996) (*Preprint* hep-ph/9606419)
[14] Mahlon G and Parke S J, *Phys. Lett.* B **411**, 173 (1997) (*Preprint* hep-ph/9706304)
[15] Uwer P, *Phys. Lett.* B **609**, 271 (2005) (*Preprint* hep-ph/0412097)
[16] Fajfer S, Kamenik J F and Melić B, JHEP **1208** (2012) 114 (*Preprint* arXiv:1205.0264 [hep-ph])
[17] Bernreuther W and Si Z G, *Phys. Lett.* B **725**, 115 (2013) Erratum: [*Phys. Lett.* B **744**, 413 (2015)] (*Preprint* arXiv:1305.2066 [hep-ph])